

## Scaling Regime of Spiral Wave Propagation in Single-Diffusive Media

Alain Karma

*Physics Department, Northeastern University, Boston, Massachusetts 02115*

(Received 30 August 1991)

We report uniformly scaling rotor solutions of the free-boundary problem of wave propagation in reaction-diffusion models of single-diffusive excitable-oscillatory media with a unique wavelength and rotation frequency obeying the Fife scaling  $\lambda \sim \epsilon^{2/3}$  and  $\omega \sim \epsilon^{-1/3}$ . In simulation of the models, the small- $\epsilon$  rotation regime appears to always be non-steady-state but, remarkably, it remains partially describable in terms of these solutions.

PACS numbers: 82.40.Fp, 87.90.+y

Spiral wave propagation has come to be recognized as an important spatiotemporal behavior observed in a wide range of excitable and oscillatory media of physical, chemical, and biological origin [1]. The fundamental interest in these waves, in the broad context of pattern formation, and their relevance to human health, in the context of the heart muscle [1], have jointly contributed to trigger a growing interdisciplinary effort to understand their propagation.

Theoretical investigations of spiral waves have been conducted predominantly in two-variable reaction-diffusion (RD) models. The FitzHugh-Nagumo (FHN) model,

$$\epsilon \frac{\partial u}{\partial t} = \epsilon^2 \nabla^2 u + 3u - u^3 - v, \quad (1)$$

$$\frac{\partial v}{\partial t} = u - \delta - \gamma v, \quad (2)$$

is one of the simplest caricatures of single-diffusive (no  $v$  diffusion) excitable-oscillatory media which, despite its simplicity, already captures many intricate features of spiral wave behavior (for a recent survey see Ref. [2]). In this model,  $\epsilon$  is the usual small parameter characterizing the abruptness of excitation,  $\gamma$  is a fixed parameter of order unity, and  $\delta$  (varying in the interval  $[-\sqrt{3}, 0]$ ), controls the properties of the medium: excitable (oscillatory) with a stable (unstable) spatially homogeneous fixed point of the system (1),(2) (by symmetry the intervals  $[-\sqrt{3}, 0]$  and  $[0, \sqrt{3}]$  are equivalent).

Over the years, two central theoretical problems concerning rigidly rotating spiral waves (rotors) have attracted particular attention. The first, the problem of selection, has been to understand how to predict the uniquely observed rotor shape and angular frequency  $\omega$  of shape-preserving rotation. The second, the problem of scaling, has been to understand how the overall size and frequency of rotors scale with the small parameter  $\epsilon$ . These two problems have been investigated theoretically within a free-boundary (FB) formulation of spiral wave propagation [3,4] which follows from the singular nature of the two-dimensional  $u$ -field profile in the small- $\epsilon$  limit.

Fife [3] conjectured that there should be a unique solution to this problem which corresponds to the rotor observed in numerical simulation of RD models. Further-

more, using general scaling arguments, he proposed that the frequency and wavelength of rotors should scale, respectively, as  $\epsilon^{-1/3}$  and  $\epsilon^{2/3}$  in the  $\epsilon \rightarrow 0$  limit. More recently, Pelce and Sun [5] solved the FB problem for a piecewise-linear single-diffusive RD model and demonstrated for the first time explicitly the existence of smooth rotor solutions (no discontinuities) rotating around an effective hole of radius  $R$ . Since the solutions of these authors were obtained numerically over a restricted range of  $\epsilon$ , the questions remained as to whether these smooth solutions persisted in the  $\epsilon \rightarrow 0$  limit where the FB formulation is supposed to be valid, and as to whether the selected rotor frequency would obey Fife's scaling. In recent studies [6], we showed that solutions with a smooth core and continuous variations of  $v$  along the boundary only persist in the  $\epsilon \rightarrow 0$  limit in a parameter range  $\sqrt{3} + \delta \sim \epsilon^{1/3}$  where the kinetics of the FHN model is only weakly excitable (meaning that the threshold perturbation needed to cause an excitation is large). However, since the parameter range  $\sqrt{3} + \delta \sim \epsilon^{1/3}$  constitutes a vanishingly small portion of the entire excitable-oscillatory range  $\delta = [-\sqrt{3}, 0]$  in the  $\epsilon \rightarrow 0$  limit, the questions have remained as to what the solutions of the FB problem for arbitrary  $\delta$  become in that limit, and as to what extent they can describe numerical simulation results of single-diffusive RD models. There is presently a particularly strong motivation to examine this limit in view of the recent numerical simulation findings of Winfree for the FHN model which have shown evidence of Fife scaling and a predominance of unsteady rotation at small  $\epsilon$  [2].

In this Letter, we construct the leading-order rotor solutions to the FB problem of single-diffusive media which possess uniform scaling properties in the  $\epsilon \rightarrow 0$  limit ["uniformly scaling rotor solutions" (USRS)], and examine their connection to the underlying rotor solutions of the partial differential equation system (1),(2) (RSPDE).

We shall find that these solutions have a front and a back boundary of identical shapes (Fig. 1) separated by a finite angle  $\Delta\theta$  related to  $\delta$  by the relation

$$\Delta\theta = \pi \left( \frac{\sqrt{3} + \delta}{\sqrt{3}} \right), \quad (3)$$

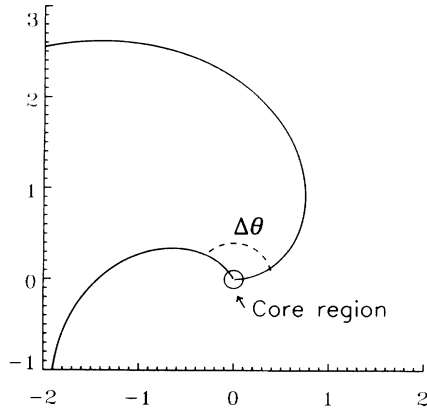


FIG. 1. Uniform rotor solution shown here for angle  $\Delta\theta = 120^\circ$ .

and have an angular rotation frequency and wavelength given by

$$\omega = \left[ \frac{\pi(3-\delta^2)}{2\sqrt{6}B} \right]^{2/3} \epsilon^{-1/3}, \quad (4)$$

$$\lambda = \left[ \frac{16\sqrt{6}\pi^2 B^4}{3-\delta^2} \right]^{1/3} \epsilon^{2/3}, \quad (5)$$

where  $B = 1.738\dots$  is a constant determined numerically. The only condition for the validity of these solutions is that  $\epsilon^{1/3} \ll \sqrt{3} + \delta$ . Consequently, USRS survive in the limit  $\epsilon \rightarrow 0$  over almost the entire excitable-oscillatory range of  $\delta$ , except in the narrow weakly excitable range  $\sqrt{3} + \delta \sim \epsilon^{1/3}$  where one must recover the smooth rotor solutions constructed previously [5,6].

We start our analysis with the well-established equations of the FB problem of rigid rotors [3-5] which, for the system (1),(2), take the form

$$c_n = c(v_b) - \epsilon \kappa, \quad (6)$$

$$\omega \frac{\partial v}{\partial \theta} + h^\pm(v) - \delta - \gamma v = 0. \quad (7)$$

Equation (6) relates the local normal velocity of the boundary, separating two regions  $\mathcal{D}^\pm$  of positive and negative  $u$ , to the local values of the slow variable  $v$  on this boundary ( $v_b$ ) and the local curvature  $\kappa$ . Equation (7) dictates the evolution of  $v$  in the two regions  $\mathcal{D}^\pm$  where the functions  $h^\pm(v)$  are implicitly defined by the largest positive root  $h^+(v)$  and smallest negative root of  $h^-(v)$  of the equation  $3u - u^3 - v = 0$  describing the  $u$  nullcline. We parametrize the rotor boundaries by the coordinates  $x = r \cos[\theta^\pm(r) - \omega t]$  and  $y = r \sin[\theta^\pm(r) - \omega t]$ , where the  $+$  and  $-$  signs refer to the front and back boundaries.

To construct the solution we first derive explicit expressions for  $v_b$  on the front ( $v_b^+$ ) and back ( $v_b^-$ ). We first assume that  $v_b$  is uniformly small, which does not constitute an additional assumption since its value will self-

consistently turn out to be of  $O(\epsilon^{1/3})$  at the end of our calculation. It is easy to deduce that for small  $v$  the functions  $h^\pm(v)$  take on the asymptotic form  $h^\pm(v) = \pm\sqrt{3} - v/6 + O(v^2)$ . Substituting these forms of  $h^\pm(v)$  into Eq. (7) and writing down explicitly the equation in each region  $\mathcal{D}^\pm$  we obtain

$$\omega \frac{\partial v}{\partial \theta} = \begin{cases} -\sqrt{3} + \delta + (\gamma + \frac{1}{6})v & (\mathcal{D}^+), \\ \sqrt{3} + \delta + (\gamma + \frac{1}{6})v & (\mathcal{D}^-). \end{cases} \quad (8)$$

$$\omega \frac{\partial v}{\partial \theta} = \begin{cases} -\sqrt{3} + \delta + (\gamma + \frac{1}{6})v & (\mathcal{D}^+), \\ \sqrt{3} + \delta + (\gamma + \frac{1}{6})v & (\mathcal{D}^-). \end{cases} \quad (9)$$

We can neglect the terms of order  $v$  in Eq. (8) since by assumption  $v$  is small compared to unity. This can always be done in Eq. (8) since  $\delta$  varies over the range  $[-\sqrt{3}, 0]$ . However, in Eq. (9) the terms of order  $v$  can only be neglected as long as  $\sqrt{3} + \delta \gg v$ . Since  $v$  turns out to be of  $O(\epsilon^{1/3})$ , it is precisely this constraint which in the end will imply that the solutions we derive here are valid only in the range  $\epsilon^{1/3} \ll \sqrt{3} + \delta$ . Next, integrating Eq. (8) from  $\theta^-$  to  $\theta^+$  and Eq. (9) from  $\theta^+$  to  $2\pi + \theta^-$  we obtain at once the expressions

$$v_b^- = v_b^+ + [(\sqrt{3} - \delta)/\omega](\theta^+ - \theta^-), \quad (10)$$

$$v_b^+ = v_b^- - [(\sqrt{3} + \delta)/\omega][2\pi - (\theta^+ - \theta^-)]. \quad (11)$$

It then follows that Eqs. (10) and (11) only have solutions if  $\Delta\theta \equiv \theta^+ - \theta^-$  and  $v_b^\pm$  have constant values given, respectively, by Eq. (3) and  $v_b^\pm = \mp \pi(3 - \delta^2)/2\sqrt{3}\omega$ . Also, from the constancy of  $\Delta\theta$ , it follows that the front and back boundaries must have identical shapes. We only need to consider one of the two boundaries to complete our solution and arbitrarily choose the front boundary. We express Eq. (6) in terms of the variable  $\Psi^+ \equiv r d\theta^+/dr$  and use the small- $v$  expression for the plane-wave velocity  $c(v_b^+) = -v_b^+/\sqrt{2} + O((v_b^+)^3)$ , which is easily derivable [4]. Furthermore, we perform the scale transformations  $\omega = \Omega \epsilon^{-1/3}$  and  $\rho = \sqrt{\Omega} \epsilon^{-2/3} r$ . After simple algebraic manipulations Eq. (6) can be transformed to the final  $\epsilon$ -independent form:

$$\frac{d\Psi^+}{d\rho} = \rho(1 + \Psi^{+2}) - B(1 + \Psi^{+2})^{3/2} - \frac{\Psi^+(1 + \Psi^{+2})}{\rho}, \quad (12)$$

where  $B \equiv (3 - \delta^2)\pi/2\sqrt{6}\Omega^{3/2}$ . Equation (12) is identical in form to the equation of Burton, Cabrera, and Frank governing the growth of screw dislocations on crystal surfaces [4,7]. It results here from the requirement that for USRS to exist  $v$  must be constant along the front and back boundaries [Eqs. (10) and (11)]. The solutions of Eq. (12) satisfying the boundary conditions  $\Psi^+(0) = 0$  and  $\Psi^+(r) \sim r$  for  $r \rightarrow \infty$  can easily be shown by shooting to exist for a unique value of  $B = 1.738$ . From the expression for  $B$  and the definition  $\omega = \Omega \epsilon^{-1/3}$ , we obtain at once the scaling result (4). It also follows that  $v_b^\pm \sim \epsilon^{1/3}$  and from the asymptotic form of Eq. (12) that  $\lambda = 2\pi B \epsilon^{2/3}/\sqrt{\Omega}$  [Eq. (5)]. Finally, although for clarity of

exposition we have derived our results for the FHN model, they can be extended to other single-diffusive RD models [8].

The USRS have both a slope discontinuity (SD) along the boundary (except for  $\Delta\theta=\pi$ ) and a discontinuity of  $v$  at the origin. These singularities could appear at first to be incompatible with the RSPDE which must be continuous, as viewed previously [4]. However, there is no *a priori* incompatibility since these solutions only describe the shape of the boundary between  $\mathcal{D}^+$  and  $\mathcal{D}^-$  on a scale of  $O(\epsilon^{2/3})$  which, in the  $\epsilon \rightarrow 0$  limit, is much larger than the small core region of size  $\epsilon$  around the origin, within which both  $u$  and  $v$  have rapid spatial variations. To establish the existence of RSPDE one needs to determine if the solution of the PDE on the scale  $\epsilon$  of the core can be matched to the USRS on the scale  $\epsilon^{2/3}$ . In the case  $\Delta\theta=\pi$ , where no SD arise, this core solution is simply derivable analytically and given in polar coordinates  $(r, \phi = \theta - \omega t)$  by  $u = \sqrt{3} \tanh(\sqrt{3/2} r \cos \phi / \epsilon)$ , which satisfies trivially the no SD boundary condition of the USRS at the origin, and  $v = -\epsilon^{1/3} \Omega^{-1} \int_0^\phi u(r, \phi') d\phi'$  which matches smoothly onto the solution of Eqs. (10) and (11) in the limit  $r/\epsilon \rightarrow \infty$ . It should be noted that, although benign, the small core can generate significant higher-order corrections of order  $\epsilon^{1/3}$  to the shape and frequency of RSPDE that will be treated elsewhere [9]. In the more generic case where SD are present ( $\Delta\theta \neq \pi$ ), the existence of core solutions remains to be established. However, what can be stated with certainty is that, if these solutions exist, then the RSPDE should have a shape which corresponds on the large scale [of  $O(\epsilon^{2/3})$ ] to the USRS with a frequency and wavelength given, respectively, by Eqs. (4) and (5). This represents one of the most interesting aspects of our results with regard to spiral pattern selection: The dynamics of the short scale ( $\epsilon$ ) is tied to that of the large scale ( $\epsilon^{2/3}$ ) and the effect of the core on frequency and shape selection is benign in the  $\epsilon \rightarrow 0$  limit.

To explore the connection between the USRS and the full rotor dynamics of the PDE, we have compared the analytical results with the numerical simulation results of Winfree [2] which span a wide portion of the parameter plane  $(\delta, \epsilon)$  of the FHN model, also including a few additional data points from our own simulations which extend to smaller  $\epsilon$  in the case  $\delta=0$ . It is apparent from Fig. 2 that, in the case  $\Delta\theta=\pi$ , the observed  $\omega$  are in relatively good quantitative agreement with the analytical prediction and the expected scaling behavior. This agreement persists even at smaller values of  $\epsilon$  where rotation becomes non-steady-state (most likely due to the characteristic meandering oscillatory instability of RSPDE [10]). This is consistent with the observation that near  $\Delta\theta=\pi$  the amplitude of meander (measured as the diameter of a circle enclosing the excursions of the tip) remains at least 1 order of magnitude smaller than the rotor wavelength and, thus, has a minimal effect on the rotation frequency. In Fig. 3, it is apparent that away

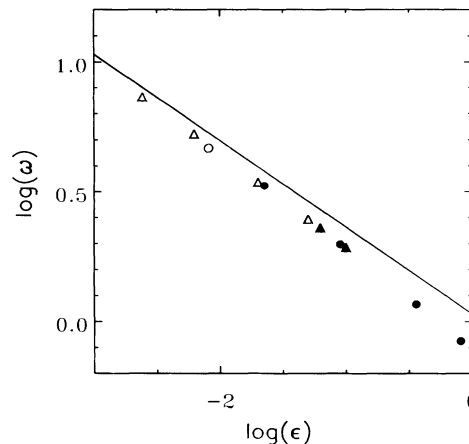


FIG. 2.  $\log(\omega)$  as a function of  $\log(\epsilon)$  for the case  $\delta=0$ . The solid line corresponds to the analytic prediction for  $\omega$  [Eq. (4)], the circles to the numerical simulation results of Ref. [2] for the FHN model (1),(2) with  $\gamma = \frac{1}{2}$ , and the triangles to our numerical results of the same model with  $\gamma=0$ . Note that Eq. (4) does not depend on  $\gamma$  so that both sets of results can be used. The solid symbols (circles or triangles) correspond to steady-state rotors while open symbols correspond to non-steady-state rotors. In the case of non-steady-state rotation, an "average  $\omega$ " is computed from a value of the period averaged over several rotation cycles.

from  $\Delta\theta=\pi$  ( $\delta \neq 0$ ) the agreement between analytics and numerics becomes poorer, in particular at smaller  $\epsilon$ . This in turn is consistent with Winfree's observation that the amplitude of meander increases dramatically with increasing  $|\delta|$  and decreasing  $\epsilon$ , becoming comparable to  $\lambda$ . As  $|\delta|$  is increased further, the weakly excitable limit  $\sqrt{3} + \delta \sim \epsilon^{1/3}$  is eventually reached where stable [11] rotor solutions with smooth cores exist [5,6].

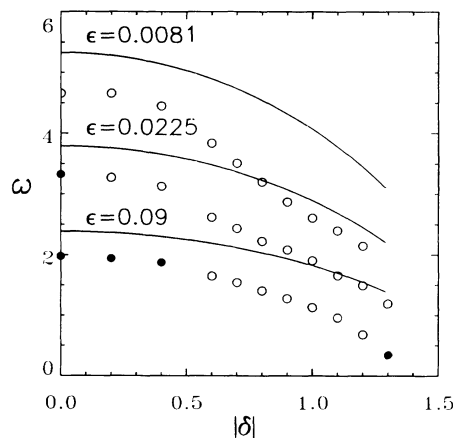


FIG. 3.  $\omega$  as a function of  $|\delta|$  for three values of  $\epsilon$ . The solid lines correspond to the analytic prediction for  $\omega$  [Eq. (4)] and the circles to the numerical simulation results of Ref. [2]. Solid (open) circles correspond to steady-state (non-steady-state) rotation.

To conclude we note that the USRS provide exact leading-order-in- $\epsilon$  analytical predictions of wavelength and frequency of spiral patterns that should be applicable to a wide range of experimental systems described by the single-diffusive reaction-diffusion equation [8]. These predictions should be most accurate at small  $\epsilon$  and in parameter ranges corresponding to  $\Delta\theta$  near  $\pi$ . Away from this range, they still provide a good estimate despite the predominance of non-steady-state rotation. Surface reactions [12], where concentration spiral patterns can be accurately studied and  $\epsilon$  is especially small, are perhaps the best characterized single-diffusive systems in which to test these predictions.

I wish to thank M. Cross, P. Fife, D. Kessler, H. Levine, P. Pelce, J. Sun, V. Hakim, and A. Winfree for helpful exchanges. I am particularly grateful to A. Winfree for communicating to me his numerical results ahead of publication. They have motivated this study and provided the valuable data base for the comparison presented in Figs. 2 and 3. Acknowledgment is made to the Donors of the Petroleum Research Fund for the support of this research.

---

[1] R. J. Field and M. Burger, *Oscillations of Travelling Waves in Chemical Systems* (Wiley, New York, 1985); A. T. Winfree, *When Time Breaks Down* (Princeton Univ. Press, Princeton, 1987); V. S. Zykov, *Simulation of Wave Processes in Excitable Media* (Manchester Univ. Press, New York, 1987).

- [2] A. T. Winfree, *Chaos* **1**, 303 (1991).  
 [3] P. C. Fife, *J. Stat. Phys.* **39**, 687 (1985); *CBMS-NSF Conf. Ser. Appl. Math.* **53**, 1-93 (1988).  
 [4] J. P. Keener, *SIAM J. Appl. Math.* **46**, 1039 (1988); J. J. Tyson and J. P. Keener, *Physica (Amsterdam)* **32D**, 327 (1988).  
 [5] P. Pelce and J. Sun, *Physica (Amsterdam)* **48D**, 353 (1991).  
 [6] A. Karma, *Phys. Rev. Lett.* **66**, 2274 (1991); in *Non-linear Phenomena Related to Growth and Form*, edited by M. Ben Amar, P. Pelce, and P. Tabeling (Plenum, New York, 1991).  
 [7] W. K. Burton, N. Cabrera, and F. C. Frank, *Philos. Trans. R. Soc. London, Ser. A* **243**, 299 (1951).  
 [8] For models of the form  $\epsilon\dot{u} = \epsilon^2\nabla^2u + f(u,v)$  and  $\dot{v} = g(u,v)$ , Eqs. (3)-(5) become, respectively,  $\Delta\theta = 2\pi g^- / (g^- - g^+)$ ,  $\omega = \{\alpha\pi g^+ g^- / [(g^- - g^+)B]\}^{2/3} \epsilon^{-1/3}$ , and  $\lambda = 2\pi^2\alpha\omega^{-2} g^+ g^- / (g^- - g^+)$ . The three constants  $\alpha$  and  $g^\pm$  are defined, respectively, by the plane-wave velocity relation  $c(v) = \alpha(v - v^*)$  (for  $v$  close to the stall value  $v^*$ ) and  $g^\pm = g(h^\pm(v^*), v^*)$ .  
 [9] A. Karma and V. Hakim (to be published).  
 [10] For recent experimental and theoretical studies of meander, see Ref. [2]; S. C. Müller, T. Plesser, and B. Hess, *Physica (Amsterdam)* **24D**, 87 (1987); W. Jahnke, W. E. Skaggs, and A. T. Winfree, *J. Phys. Chem.* **93**, 740 (1989); G. S. Skinner and H. L. Swinney, *Physica (Amsterdam)* **48D**, 1 (1991); E. Lugosi, *Physica (Amsterdam)* **40D**, 331 (1989); D. Barkley, M. Kness, and L. Tuckerman, *Phys. Rev. A* **42**, 2489 (1990); A. Karma, *Phys. Rev. Lett.* **65**, 2824 (1990).  
 [11] P. Pelce and J. Sun, *Phys. Rev. A* **44**, 7906 (1991).  
 [12] S. Jakubith, H. H. Rotermund, W. Engel, A. von Oertzen, and G. Ertl, *Phys. Rev. Lett.* **65**, 3013 (1990).